Tellus (1988), *40B*, 134–147

Deuterium in water vapor above the atmospheric boundary layer

By STANLEY DAVID GEDZELMAN, *Department of Earth and Planetary Sciences, City College of New York, Convent Avenue and 138th Street, New York, NY 10031, USA* and *Lamont-Doherty Geological Observatory of Columbia University, Palisades, NY 10964, USA*

(Manuscript received 14 May 1986; in final form 14 April 1987)

ABSTRACT

A model for the isotopic composition of water vapor above the atmospheric boundary layer is presented. The model includes the effects of isotope fractionation and vertical turbulent transport of vapor. It utilizes an assumed air trajectory in which an air parcel initially acquires water vapor over the ocean, rises dry and then moist adiabatically, and finally sinks to the observed conditions of height, temperature and dew point temperature. Discrepancies between model predictions and actual profiles are shown to have characteristic signatures which render the isotopic composition of water vapor of potential value as a dynamic tracer of atmospheric processes and motions.

1. Introduction

Knowledge of the stable isotopic composition of atmospheric water vapor is a prerequisite for explaining both the meteorological and climatological signals that have been obtained from isotopic studies of precipitation, tree rings and ice cores. Despite this, there are only two extensive data sets for the isotopic composition of water vapor above the atmospheric boundary layer. Taylor (1972) and Ehhalt (1974) measured the deuterium to hydrogen (D/H) ratios, expressed in terms of the quantity, δD, of atmospheric water vapor for a number of vertical profiles. By definition,

$$\delta D = \left[\frac{(D/H)_{\text{sample}}}{(D/H)_{\text{SMOW}}} - 1 \right] 1000$$

where SMOW is Standard Mean Ocean Water. (Throughout this paper all δD values are expressed in parts per thousand.) All samples were collected in cloud-free air to avoid contamination by cloud droplets. Taylor (1972) documented a general decrease of δD values with altitude through the lower and mid troposphere. He pointed out a high correlation between the isotopic ratios and the specific humidity of the air, a finding corroborated at the surface by White and Gedzelman (1984).

The fundamental physical mechanism that accounts for this behavior was shown by Dansgaard (1953) to be the fractionation of heavy isotopes during condensation. As saturated air rises, the heavy isotopes condense more readily due to their lower equilibrium vapor pressures, so the δD value of the remaining vapor decreases monotonically.

This basic process is complicated by a number of physical and meteorological factors. Dansgaard (1954) showed the vertical and temporal variations of $\delta^{18}O$ values of the vapor also depend on the prior history of the air parcels and on turbulent mixing. White and Gedzelman (1984) showed further how δD values at the surface vary with the synoptic meteorological setting and with the static stability both in and above the atmospheric boundary layer. Cloud microphysical processes such as the nature of the phase change, the retention of cloud droplets in the cloud, and interactions between the vapor and raindrops falling from above also affect the isotopic composition of the vapor (see e.g.,

Dansgaard, 1964; Miyake et al., 1968 and Rozanski and Sonntag, 1982).

Ehhalt et al. (1980) showed furthermore that not all profiles exhibit a simple decrease of δD values with altitude. A number of flights were conducted to greater heights and on average, δD values began to increase in the upper troposphere, sometimes despite continued decrease of specific humidity. Ehhalt's (1974) data also reveal a few mid and upper tropospheric layers with anomalously high δD values characteristic of vapor at sea level, thus suggesting that under certain conditions water can be transported to great heights without undergoing significant fractionation.

The purpose of this paper is to explain the vertical and temporal variations of δD values above the atmospheric boundary layer in terms of the dominant physical processes and the prevailing meteorological conditions. A simple model is presented that accounts for a large percentage of the variance of the δD values in the lower half of the troposphere. The unique feature of this model is that it predicts δD values by reconstructing a separate air parcel trajectory for each level in a vertical profile from the observed values of pressure, temperature and specific humidity. The effects of transport of vapor aloft by turbulent mixing and retention of liquid water within the cloud are also incorporated and evaluated. Observed δD values are then compared to the model results and are discussed in terms of the meteorological situation.

2. The model

The general equation of the isotopic model used in this paper is

$$\frac{dR_v}{R_v} = \frac{(1-\alpha)\,dX - AX\,d\alpha}{1 + X(\alpha A - 1)} \qquad (1)$$

which was first obtained by Merlivat and Jouzel (1979) in a slightly different form. Here, R is the fraction of heavy molecules and α is the fractionation factor. X is the fraction of vapor that has condensed from the air parcel. A is the fraction of condensed vapor that remains with the parcel in the form of cloud droplets, which are assumed to be in isotopic equilibrium with the vapor.

Results for different values of A, previously given in Jouzel (1979), are presented in Fig. 1. This illustrates how the retained liquid water in the cloud acts as a buffer to slow the rate of decrease of δD values as condensation proceeds.

Two simple, limiting cases of eq. (1) are often considered. The first is the Rayleigh condensation or open system model in which $A = 0$ and no interaction is allowed between vapor and precipitation particles after their formation. Due to the extremely low diffusion of molecules within ice, the assumptions involved in the Rayleigh condensation model are largely satisfied for snow situations. The second limiting situation is the closed system model, $A = 1$, in which all cloud and precipitation particles are retained and equilibrate instantly with the vapor. This is the model used in the early isotopic studies on hail (Facy et al., 1963; see also Knight et al., 1981).

In this paper, condensation is assumed to result from moist adiabatic ascent (see e.g., Fleagle and Businger, 1980) although the sensitivity of δD values to radiative temperature changes is evaluated in Section 3. Since the fractionation factor is not constant, δD values must be calculated iteratively using eq. (1).

The fractionation factor, α, depends on the temperature and the nature of the phase change.

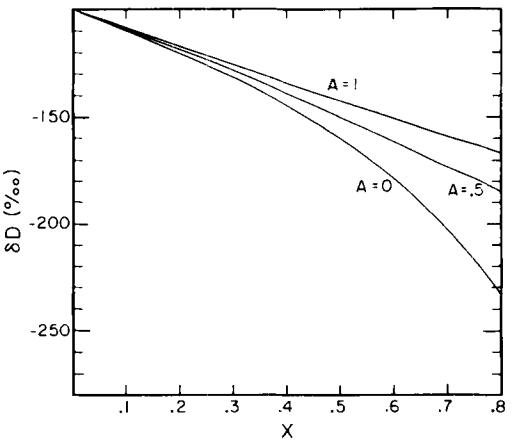

Fig. 1. δD values of atmospheric water vapor as a function of percentage of vapor condensed, X, for various percentages of retained cloud water, A. The Rayleigh condensation or open system model is $A = 0$ while the closed system model is $A = 1$. The fractionation factor, α, for these curves is assumed to be constant.

For liquid–vapor phase changes (α_{evap}) we use Majoube's (1971) expression for the experimentally determined equilibrium fractionation factor, while for solid–vapor phase changes (α_{sub}) we use the expression based on experiments of Merlivat and Nief (1967).

At temperatures below 0°C, the percentage of vapor condensing onto ice varies from cloud to cloud (Mason, 1971; Pruppacher and Klett, 1980). In general, as the temperature decreases both the fraction of frozen cloud particles and the relative difference between saturated vapor densities of ice and water increase so that the percentage of vapor condensing onto ice particles increases. We therefore arbitrarily impose the condition that the percentage of vapor condensing onto ice increases linearly from 0% at 0°C to 100% at and below −15°C. For the intermediate temperature range, α is given by,

$$\alpha = (\alpha_{sub} - \alpha_{evap})(273.16 - T)/15 + \alpha_{evap}, \quad 258 < T < 273. \tag{2}$$

The reduction of α_{sub} associated with supersaturated conditions with respect to ice at low temperatures (Jouzel and Merlivat, 1984) was not taken into account. Because the microphysical conditions can differ from cloud to cloud we calculate the sensitivity of δD values to changes in α in Section 3.

The model presented here accords with the nature of the existing data sets of the isotopic composition of atmospheric water vapor, none of which had upwind measurements of δD values or cloud microphysical properties. It is then necessary to make assumptions about the history of the air parcels. Most of the data were collected under fair weather conditions in which the air was subsaturated. The low humidities and δD values suggested that the air had previously undergone significant condensation and fractionation and subsequently sunk to the observed level.

The simplest model that can account for these properties consists of the hypothetical trajectory shown in Fig. 2. The air is assumed to be initially charged with vapor over the ocean. Its initial relative humidity is assumed equal to 80% and is chosen in such a manner that the Lifting Condensation Level (LCL) occurs at 960 mb. Such values are considered reasonable for air over the sea surface (Merlivat and Jouzel, 1979). The sensitivity of δD values to changes of the LCL is considered in Section 4. The initial δD value is then obtained using the expression,

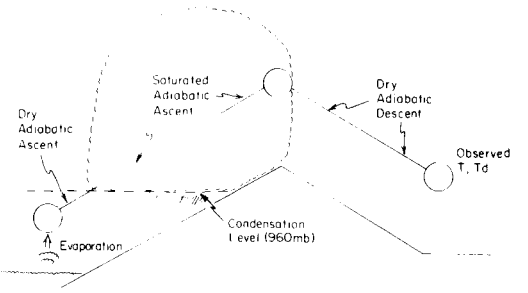

Fig. 2. The model trajectory. Air measured at far right is presumed to derive from the ocean, thereafter rising dry and then moist adiabatically and finally sinking to the observation point. Vapor may be added to the air by turbulent transport after condensation has taken place.

$$\delta D_0 = \left[\frac{1}{\alpha}\frac{1-k}{1-kh} - 1\right] 1000 \tag{3}$$

of Merlivat and Jouzel (1979), where h is the relative humidity and $k = 0.005$.

The air is assumed to rise dry adiabatically until the LCL and thereafter moist adiabatically. In the final part of the trajectory the air is assumed to sink dry adiabatically to the observed level. Taylor (1984) has pointed out that δD values are seriously overestimated when the effects of sinking in unsaturated air are neglected.

The model calculations are first performed backwards in time in order to obtain both the topmost point of the trajectory and the initial temperature and δD values at the sea surface. Once the initial values are obtained the air is taken forward through its trajectory, numerically calculating all changes of T, q, and δD values. The calculations are performed separately for each level in the sounding so that the initial specific humidity, q_0 and isotopic composition, δD_0 are not assumed uniform. The model is therefore able to predict δD profiles for soundings that contain air from widely separated source regions.

This approach helps demonstrate why a sounding need not exhibit a simple $\delta D - q$ relation. Taylor (1972) observed that there is a single $\delta D - q$ relation only when the air at all levels in the sounding has a similar origin. If, on the other

hand, the sounding consists of two or more distinct airmasses, each exhibits a different $\delta D - q$ relation.

The model is run for the full range, $0 \leqslant A \leqslant 1$, i.e., from the Rayleigh condensation (open system) to the closed system models limits, so long as the parcel remains warmer than $-15°C$. Once the parcel temperature falls below $-15°C$, we assume precipitating clouds consist entirely of ice particles and automatically set $A = 0$.

Turbulent transport of vapor acts to reduce the vertical gradient of δD values by mixing the air. Its effects are incorporated in the model by modifying the idealized approach taken by Eriksson (1965), who showed that for a thoroughly mixed atmosphere in steady state, the fractionation factor, α, should be replaced by $\alpha^{0.5}$ in all calculations regarding the vertical profile of δD.

The atmosphere is not often either fully mixed or totally unmixed. The degree to which the atmosphere is mixed subsequent to condensation depends on (1), the time that has elapsed since the precipitation ended and (2), the turbulent diffusion coefficient, K. Typical values for K in the free atmosphere vary between 10^1 and 10^2 $m^2\ s^{-1}$ (Liu et al., 1984) and depend on such factors as the static stability and vertical wind shear. Using this range of values, we find the vapor adjusts to a thoroughly mixed state with a typical relaxation time between about 1 and 10 days. On extremely unstable days with a strong jet stream the atmosphere can mix within a matter of hours while during very stable periods with small vertical wind shear, the mixing time can be several weeks.

Taylor (1972, 1984) found that for most of the profiles collected under anticyclonic conditions the atmosphere was essentially unmixed. These samples were collected around Mannheim, Germany under mostly stable atmospheric conditions where little mixing would be expected. A number of Ehhalt's profiles, such as the summer samples collected over Scottsbluff, Nebraska and Death Valley, California, were statically unstable and consequently well mixed.

The model was run twice for each sounding—once for the fully mixed case and once for the unmixed case. We found that, depending on the static stability, one or the other of these two extreme cases usually fit the observed data well. The measure of stability used is the Showalter Stability Index (SSI), which is the temperature of the ambient air at 500 mb minus the temperature of a parcel lifted from the 850 mb level dry adiabatically until the point of saturation and moist adiabatically thereafter. Negative values of SSI denote unstable stratification. We found that when the SSI was less than 2 the fully mixed assumption worked well; for greater values of SSI the unmixed version led to accurate results. As might be expected, model results are more accurate for stable soundings since invariable complications due to turbulent mixing are minimized.

One of the main sources of large discrepancies between model predictions and observed δD values is the transport aloft and subsequent reevaporation of hydrometeors, as by thunderstorms. This additional vapor has seldom been subjected to much fractionation and therefore can arrive at great heights with a much higher δD value than that of the surrounding vapor. In the upper troposphere, where specific humidities tend to be very low, the injection of even small quantities of water vapor can raise δD values significantly. We have found, perhaps for this reason, that model δD predictions are often too low whenever specific humidities fall to less than about 10% of their maximum value even when the fully mixed, closed system assumptions are used.

For some of the colder samples the discrepancy between observed and predicted δD values might have resulted from incomplete collection of the vapor. This can lead to serious errors when the specific humidity is very low, as in the upper troposphere (see e.g., Pollock et al., 1980). If the vapor is not all condensed, δD measurements will be too high because of incomplete fractionation. This error can approach 1000 $(\alpha - 1)$. Most of the vapor was collected by running the air through a cold bath of dry ice, but for a few flights conducted to greater heights, Ehhalt (1974) used liquid nitrogen in the cold bath. There was an overlapping range of heights (6000–8000 m) for the two series of flights (the dry ice vs the liquid nitrogen flights) for which δD could be compared. We noticed that when the liquid nitrogen bath was used the δD values averaged about 150 lower for a given specific humidity than when dry ice was used. Therefore, we compare model

predictions with actual δD values only when $q > 0.5$ g kg^{-1} if the dry ice bath was used and $q > 0.2$ g kg^{-1} if the liquid nitrogen bath was used.

3. Sensitivity tests

We now consider the sensitivity of δD predictions to changes in the basic parameters and assumptions of the model. All results are shown in Table 1 and, unless otherwise stated, refer to the Rayleigh condensation model. Sensitivities to percent of retained cloud droplets and effects of turbulent transport will be considered in Section 4.

Consider first the effect of changing the initial condensation level, normally set at 960 mb. Lowering cloud base also lowers δD because it implies the air was initially more humid and underwent a greater degree of condensation. The sensitivity of δD values to a change of cloud base is only about 1–3‰ per 10 mb. This shows that model results are basically free from any tuning with regard to cloud base and also that δD values are not strongly dependent on the precise air trajectory within the atmospheric boundary layer.

There is also some uncertainty concerning the pressure at which the observations were taken because only aircraft altitude was given and station pressure was not recorded. Pressure at the observation level was calculated hydrostatically from actual sea level pressure when known and mean sea level pressure otherwise. Lowering the estimated pressure at observation level also lowers δD values because it implies the air rose to greater heights and underwent more condensation. A change of 10 mb results in a δD change of about 3‰. Since most observations were taken under anticyclonic conditions, calculated δD values should exhibit on average a small negative bias generally less than 5‰.

Radiative temperature changes cannot be incorporated into the model without performing actual trajectories. On average, clear air in the mid troposphere cools radiatively by about 1 °C per day (see, e.g., Covey and Haagenson, 1984), thereby decreasing the difference between the temperature and dew point temperature. This makes the model underestimate the maximum height attained by the parcel and so results in an overestimate of δD values. The sensitivity of this effect is not very large—a change of 1 °C results in a δD change of about 3‰ assuming constant specific humidity. The resultant error in δD should then not exceed 20‰ unless the vapor source region were quite remote.

Humidity measurements in the mid and upper troposphere are subject to error because the air is typically quite dry and because the humidity field in this dry air often has high spatial variability.

Table 1. *Sensitivity of δD predictions to changes in model parameters: all δD values are given in parts per thousand*

Basic state				Calculated D change due to perturbation				
T	P	q	δD	Cloud base (mb) +10/−10	P_{obs} +10/−10	T (°C) +1/−1	RH (%) +1/−1	Hydrometeor phase liquid/ice
10	700	4.43	−173.15	−1.43 1.52	1.91 −1.91	−1.67 1.65	2.10 −2.11	0.87 −4.01
−5	700	1.50	−249.09	−2.07 2.10	3.03 −3.02	−2.77 2.79	2.78 −2.87	11.28 −7.74
−20	700	0.368	−366.23	−2.91 3.01	4.48 −4.39	−4.21 4.38	3.07 −3.14	29.11 −4.08
−20	500	0.515	−400.46	−1.46 1.46	3.42 −3.44	−2.33 2.38	2.97 −3.05	27.68 −6.00

When measured humidity is too high, δD predictions will also be since the degree of condensation is then underestimated. Sensitivity increases with decreasing humidity but is typically about 2–3‰ per 1% error in relative humidity.

The final factor considered here is the sensitivity of δD values to the phase of the cloud hydrometeors. Increasing the percentage of ice in a cloud will always lower δD values (even for the open system model) because (1) the equilibrium fractionation factor for ice–vapor is greater than for liquid–vapor phase changes and (2) the saturation vapor pressure over ice is lower than over water. Therefore, for an equivalent amount of lifting, the ice cloud experiences a greater degree of condensation. Here we focus on the first of these effects since the specific humidity was measured. The cases of all water and all ice represent the upper and lower bounds for δD estimates while the model normally allows ice content to increase with decreasing temperature. The model therefore provides an intermediate and generally representative estimate. Table 1 shows that the difference between the two extreme cases can approach 40‰ so that it would be quite valuable to have data on the microphysical state of the cloud.

4. Model results and meteorological analysis

In this section, model calculations are presented and compared to measured δD values. We begin by analyzing some individual soundings to determine the meteorological conditions under which the model is generally valid. This is followed by a statistical analysis.

4.1. Individual soundings

The same basic format is used for all the figures of soundings presented here. The heavy line represents the observed profile of δD values while the four light lines give the model's predictions for the four extreme cases. The numerical sequence of the four cases is, from lowest to highest δD value, (1) the unmixed, open system, (2) the unmixed, closed system, (3) the mixed, open system, and (4) the mixed, closed system. The numerical sequence is identical for all points in every sounding. As a result it is possible to distinguish between the effects of retained droplets and turbulent mixing, both of which retard the decrease of δD with height. The shaded regions in each sounding denote the δD range caused by varying the percentage of retained droplets separately for the unmixed and fully mixed solutions.

Consider first the sounding of 26 July 1967 near Mannheim, Germany, shown in Fig. 3. Taylor (1972) noted that anticyclonic conditions prevailed and all air had a similar source region. The SSI for this sounding was 10.4, so that the air was quite stable and turbulent transport of vapor from the surface could be neglected. In general these are the weather conditions under which the model performs best. δD predictions for similar cases not shown here are of comparable and often greater accuracy.

At most levels, the observed δD values fall within the range of the model's solutions for the ummixed atmosphere and tend to be closer to the open system end. For such cases the unmixed Rayleigh condensation assumption is usually quite good despite its well-known limitations.

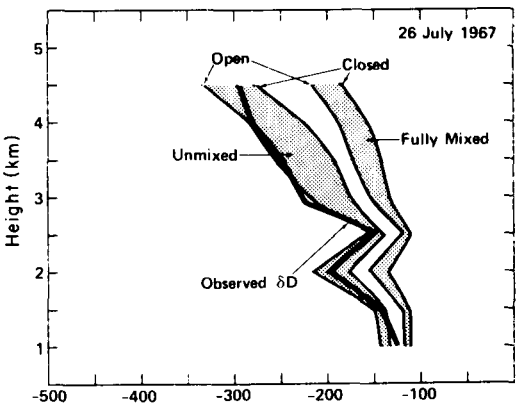

Fig. 3. The sounding of 26 July 1967 near Mannheim, Germany based on data of Taylor (1972) and showing δD values as a function of altitude. The heavy line represents observed values while the four light lines represent from lowest to highest values, the unmixed open system, the unmixed closed system, the fully mixed open system and the fully mixed closed system runs of the model. The shaded regions denote the range of solutions due to varying the percentage of retained condensate from 0% ($A = 0$) to 100% ($A = 1$). For this stable sounding taken under anticyclonic conditions the unmixed open system model predictions closely match the observed δD values and correlate 98.6%.

Only at the top and bottom of the sounding does the model yield unreliable results. Near the surface the difference between all versions of the model are smaller so that the effect of δD variations at the vapor source is relatively more important. Between 4.0 and 4.5 km, the observed gradient of δD values is much smaller than predictions based on any run of the model. A reduced or even reversed δD gradient is frequently observed in the mid and upper troposphere and may be due to the injection and reevaporation of liquid water from convective clouds (with anomalously high δD values) into the dry upper troposphere. For the same reason, model predictions, though accurate for most humid layers, are not trustworthy. For the sounding of 26 July 1967, the model accurately predicts the δD value in the humid layer at 2.5 km, indicating that the vapor in this layer did not derive from reevaporated liquid.

Consider next the sounding 24 June 1968 (also near Mannheim) shown in Fig. 4. Anticyclonic conditions also prevailed at this time and the SSI = 13.1, indicating a highly stable atmosphere. Once again, the unmixed, open system run of the model works well. One unusual feature of this sounding is that the observed values are lower than the predicted values at most levels. Taylor (1972) reported that the air had a tropical origin which implies that significant radiative cooling occurred. The sensitivity analysis of Section 3 then suggests that precipitation took place about 7 days earlier.

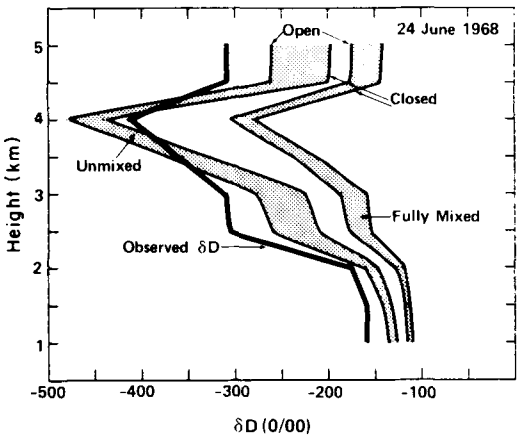

Fig. 4. The same as Fig. 3 for the stable, anticyclonic sounding of 24 June 1968, also near Mannheim. The open system model predictions again work well except for the dry layer but still correlate 97.3% with observed δD values.

The model correctly predicts that the dry layer at 4 km is associated with the lowest δD value of the sounding. Nevertheless, the predicted minimum is considerably deeper than observed. This is a characteristic feature of model δD predictions for anomalously dry layers and results from the neglect of turbulent mixing in thin layers.

Turbulent mixing invariably leads to higher δD values for a given specific humidity than a pure fractionation model indicates. This is illustrated in Fig. 5. The heavy solid curve represents the solution of the Rayleigh condensation model in terms of the specific humidity and the concentration of deuterium atoms (i.e., qR) for initial conditions $T = 20$, $P = 10^5$ Pa and $q = 10$ g kg^{-1}. The light straight lines are all lines of constant R or δD.

Consider the result of mixing two unadulterated parcels, A and B, located on the Rayleigh condensation curve. Mass balance requires that any mixture lie on some point such as C, along the straight line joining points A and B (the heavy dashed line). The essential point is that due to the nonlinearity of the Rayleigh curve, any mixture of two air parcels results in a higher δD value than one would expect for the given q on the basis of fractionation processes alone. Using point C as an example of the conditions in the mixed layer, we find that for the given value of q mixing increases the δD value from -460 to -314.

Fig. 5 can also be used to estimate the initial vapor content of an anomalously dry layer prior to any mixing with the surroundings. To do so, draw a straight line from point B (the surroundings) through point C (the observed conditions in the dry layer). Continue the line until it again touches the Rayleigh curve at point A. This represents an estimate of conditions in the dry layer prior to mixing.

Assuming all air in the anomalous layer had uniform initial potential temperature and specific humidity, q_a, and that the mixing took place after all condensation, δD of the mixture is given by a weighted average or,

$$\delta D_m = \frac{q_a \delta D_a + (q_m - q_a)\delta D_e}{q_m} \tag{4}$$

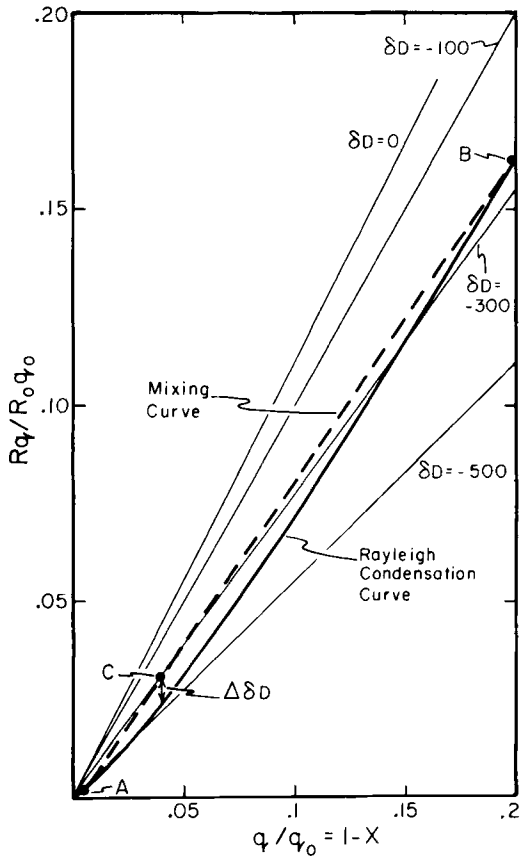

Fig. 5. δD values of atmospheric water vapor for the Rayleigh condensation model (heavy solid curve) as a function of percent of vapor remaining and percent of deuterium remaining for initial conditions, $T = 20°C$, $P = 10^5$ Pa and $q = 10$ g kg^{-1}. Light straight lines extending from the origin are lines of constant δD values. Points A and B represent two solutions to the Rayleigh condensation model, A corresponding to a dry layer and B, to the surroundings while C results from the mixing of A and B. C lies along the straight dashed line that represents all the possible mixtures of A and B. The excess of δD values above the Rayleigh solution that results from mixing, $\Lambda\delta D$, is given by the vertical line at C.

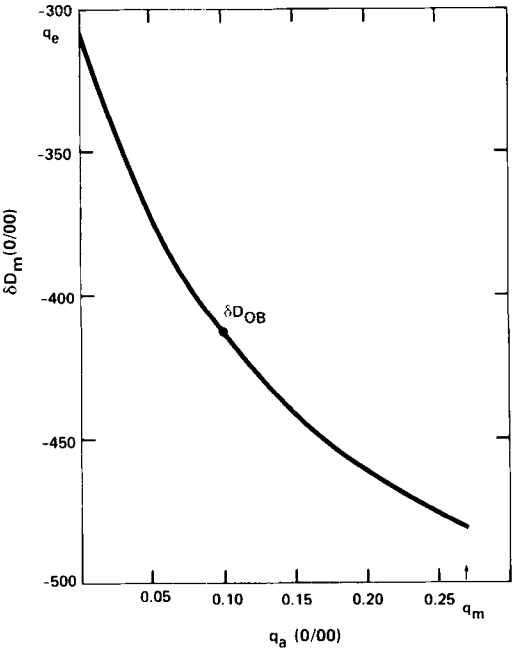

Fig. 6. The predicted δD values of the dry layer for the sounding of Fig. 4 plotted as a function of q_a, the initial vapor content of the layer prior to mixing with the surroundings. Predicted and observed values coincide for $q_a = 0.10$ g kg^{-1}.

where q_m is the observed value of q after mixing and δD_a and δD_e are the initial values of δD in the anomalous layer and the environment, respectively. When this is applied to the sounding of 24 June 1968 using $q_m = 0.269$ g kg^{-1}, the model's underestimate of δD in the dry layer due to the neglect of mixing, δD_m, is given in Fig. 6. Matching with the observed δD value in the dry layer suggests that the initial mixing ratio of the air was $q_a = 0.10$ g kg^{-1}.

Consider now the sounding of 30 June 1966 near Scottsbluff, Nebraska, shown in Fig. 7. Scottsbluff at that time was experiencing southerly winds and had a thick layer of high humidity. The SSI was -3.1 and showers were reported in the general vicinity. For this sounding the completely mixed run simulates the observed vertical gradient of δD values but predicted δD values range between 10 and 50 higher than observed at all levels. This discrepancy of about 25 between predicted and observed δD values occurred more or less consistently in the other unstable Scottsbluff soundings. It probably results from the rather high values calculated for the evapotranspired vapor when Eriksson's assumptions are used to obtain source water δD values for such an inland and elevated location.

The sounding of 24 August 1967 over Death Valley is shown in Fig. 8. Below 5.5 km, the

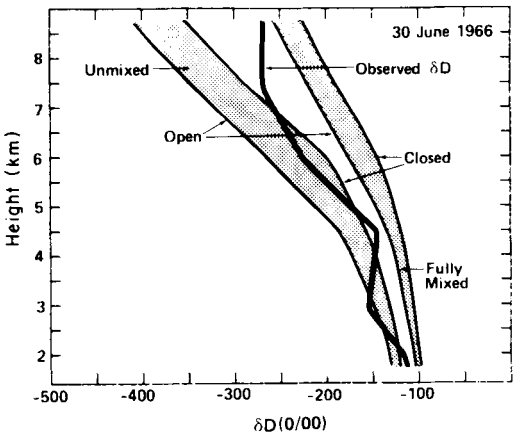

Fig. 7. Same as Fig. 3 for the unstable sounding of 30 June 1966 near Scottsbluff, Nebraska and based on data of Ehhalt (1974). For this case the fully mixed model simulates the vertical gradient of δD values but the predicted values are too low largely because the model assumes too high a δD value for the vapor added from ground level.

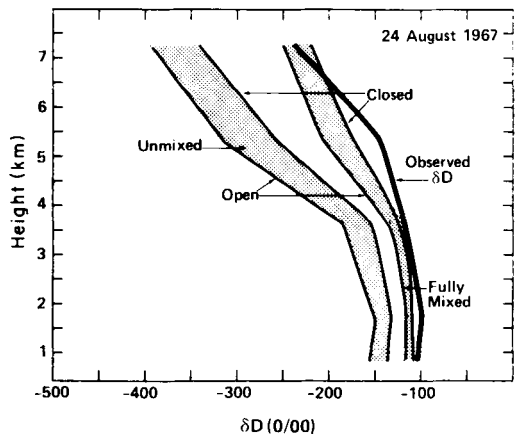

Fig. 8. Same as Fig. 3 for the unstable sounding of 24 August 1967 over Death Valley and based on data of Ehhalt (1974). Here the fully mixed model predictions work best but are higher than observed δD values.

atmosphere was unstably stratified (SSI $= -3.3$) and the fully mixed model simulates the vertical gradient of δD values well. Above 5.5 km, where the atmosphere was stably stratified, the vertical gradient of δD values is simulated by the unmixed model. At all heights, observed δD values are higher than predicted. Since the differences in the lower troposphere are not large and are not consistently seen in the other unstable Death Valley soundings, there does not appear to be a mean bias in the model's choice of source water at Death Valley.

The last individual sounding we consider is shown in Fig. 9 and was taken about 200 km west of Point Arguello, California on 22 August 1967. The remarkable feature of this sounding is the unexpectedly high δD value (-71) of the humid layer at 5500 m, which is characteristic of air at ground level and is much higher than the value predicted by the fully mixed, closed system run.

Apparently the air in this layer rose from ground level without significant change of δD values. How did this happen? The high potential temperature of 323°K calls for condensational heating during ascent from ground level but the normal fractionation processes were apparently not acting. The most likely scenario is that the humid layer resulted from outflow from the top of convective clouds. Cumulus and cumulonimbus clouds transport large quantities of water vapor and liquid water aloft and then eject them through the tops. The hydrometeors blown out of the cloud top subsequently reevaporate some distance downwind. This results in a humid layer whose δD value is closer to that of the hydrometeors, and similar to the parent vapor entering cloud base. As we have noted, Ehhalt et al. (1980) suggested that the integrated effect of

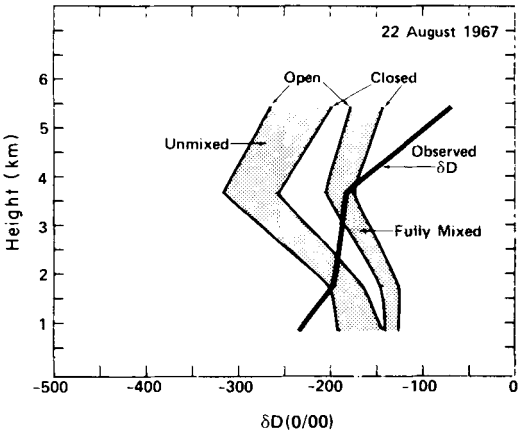

Fig. 9. Same as Fig. 3 for the sounding of 22 August 1967 near Point Arguello, California and based on data of Ehhalt (1974). Here model results fail due to injection of unfractionated water vapor in the humid layer at 5.5 km.

outflow from the tops of large thunderstorms is one of the possible mechanisms that could account for the observed average δD increase with altitude above about 10 km. Pollock et al. (1980) demonstrated that the oxidation of methane accounts for an average increase of δD values with height in the stratosphere. This may also affect the δD gradient in the upper troposphere when the air there is dry, but stratospheric specific humidities are certainly far too low to account for the high δD values of humid layers within the troposphere.

The synoptic maps also provide direct evidence that the layer at 5500 m on 22 August derived from outflow from convective cloud tops. A large number of cumulonimbus clouds were observed on the afternoon of the 21st throughout the southern half of California and Nevada, with several reports of thunderstorms around 00.00 GMT of the 22nd (see Fig. 10). This region of convective activity lay directly upwind from the observation point (indicated by the *) as the 500 mb chart of 12.00 GMT, 22 August (Fig. 11) shows. During the 24 hours preceding sampling time (19.00 GMT), a large 500 mb high was located off the California coast and the winds slowly veered from northerly to easterly, averaging about 5–10 knots. These winds were

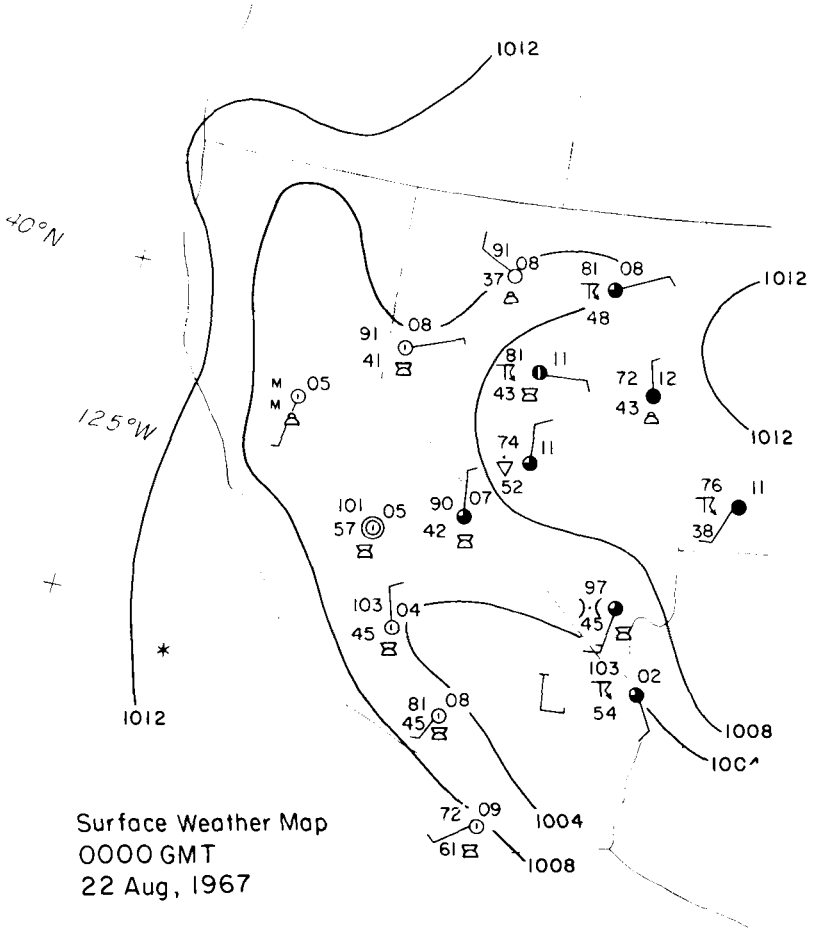

Fig. 10. Surface synoptic weather map showing numerous reports of towering cumulus and cumulonimbus clouds, for 00.00 GMT, 22 August 1967. The asterisk indicates sampling location for the vapor.

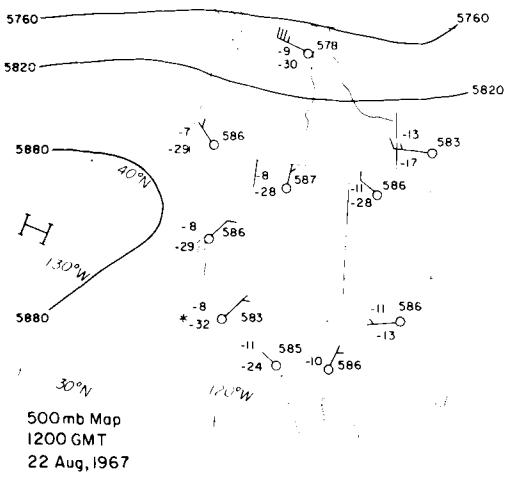

Fig. 11. The 500 mb chart for 12.00 GMT, 22 August 1967. The asterisk indicates sampling location for vapor.

adequate to transport the vapor from the convective region to the observation point by sampling time.

This case indicates that δD of water vapor can sometimes serve as a tracer of atmospheric motions. During the 61 flights conducted by Ehhalt, samples were taken only at five to ten preselected levels. Five layers in the mid or upper troposphere were observed to have high δD values (> -120) normally found only in vapor near ground level. These high δD values only occurred in layers that had a local maximum of specific humidity. For 3 of the 5 cases (despite incomplete radar coverage in the Western United States) showers or thunder showers were observed directly along the upwind trajectory. We then suggest that the likely vapor source for any humid layer in the mid or upper troposphere which has δD values characteristic of air near sea level is outflow from convective clouds. Furthermore, since Ehhalt observed only 21 anomalously humid layers, it appears that a significant percentage of all humid layers in the troposphere can be traced to this cause.

4.2. Statistical summary

We now present the overall summary of model results. The cases considered above indicate that the unmixed run of the model works best for stable soundings under anticyclonic conditions while the fully mixed run works best for soundings that are unstable or in which large-scale ascent is taking place. If a single cutoff value must be selected, SSI = 2 was found to be the optimum value. We therefore use these criteria to separate the data into two distinct categories. All data points were included unless the specific humidity fell below the threshold values discussed in Section 3 or if the layer were anomalously humid or dry (specific humidity differing by a factor greater than 2 from its surroundings). Data points below 600 mb in two of the Death Valley soundings were grouped with the unstable soundings even though SSI > 2 because the lapse rates there were dry adiabatic.

The results are summarized in Table 2. This contains the correlations between observed and predicted δD values, the r.m.s. error, bias (positive for predicted > observed) and slope, B of the regression curve for the model results. When $B < 1$, the actual variations, and usually the observed vertical gradients, of δD values are smaller than model predictions. Model predictions are shown for both open and closed systems ($A = 0, 1$). The only intermediate values of A included are 0.1 and 0.2 because results are invariably better for small A.

Table 2 shows that the unmixed run applies to the stable soundings while the fully mixed run applies to the unstable or cyclonic soundings. In addition, for both unmixed and fully mixed runs, the Rayleigh condensation model works far better than the closed system, having small bias but slightly overforecasting the variability and hence the vertical gradient of δD values.

For the stable soundings the best results correspond to $A = 0.07$. With a typical initial specific humidity of 0.01, this implies cloud liquid water contents of order 0.5–1.0 g m^{-3}, which are quite reasonable. The comparison of calculated with observed δD values for the unmixed run assuming $A = 0.1$ is shown in Fig. 12. The model overpredicts the variance and therefore vertical gradient of δD values, primarily because it cannot incorporate the decrease or even reversal of the δD gradient in the mid troposphere, which may be due to injected hydrometeors.

The results for the unstable soundings using the

Table 2. *Comparison of observed and calculated δD values*

	Stable anticyclonic points				Unstable or cyclonic points			
				Unmixed run				
A	*r*	RMSE	BIAS	*B*	*r*	RMSE	BIAS	*B*
0.0	0.906	36.6	−0.9	0.86	0.857	78.0	−60.1	0.49
0.1	0.907	36.3	7.5	0.89	0.850	70.0	−52.5	0.51
0.2	0.907	37.7	13.5	0.92	0.845	64.6	−47.0	0.53
1.0	0.901	50.1	35.2	0.98	0.826	48.6	−26.7	0.57
				Fully mixed run				
0.0	0.908	92.1	80.8	1.64	0.854	26.6	7.6	0.90
0.1	0.907	96.3	85.0	1.66	0.848	28.1	11.5	0.94
0.2	0.907	99.3	88.0	1.70	0.843	29.6	14.2	0.97
1.0	0.898	110.5	99.1	1.82	0.826	36.5	24.4	1.05

The data points are separated into two groups—the stable, anticyclonic points and the unstable or cyclonic points. Both unmixed and fully mixed runs are included and results are shown for $A = 0$, 0.1, 0.2, and 1.0. Included is the correlation coefficient, r, the slope, B, obtained from linear regression, the root mean square error, RMSE, and the bias of the predictions. Unless otherwise specified all values are given in parts per thousand. The model works best for small values of A in all cases. The fully mixed run applies well to the unstable or cyclonic soundings while the unmixed run applies well to the stable, anticyclonic soundings.

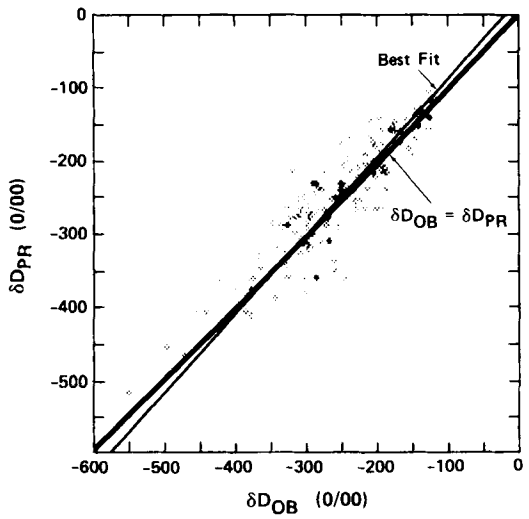

Fig. 12. Comparison of actual and predicted δD values for all acceptable points from stable, anticyclonic soundings. The model run used here is the unmixed version with $A = 0.1$. Points falling along the heavy solid line represent perfect predictions. The light solid line represents the best fit between predicted and observed values.

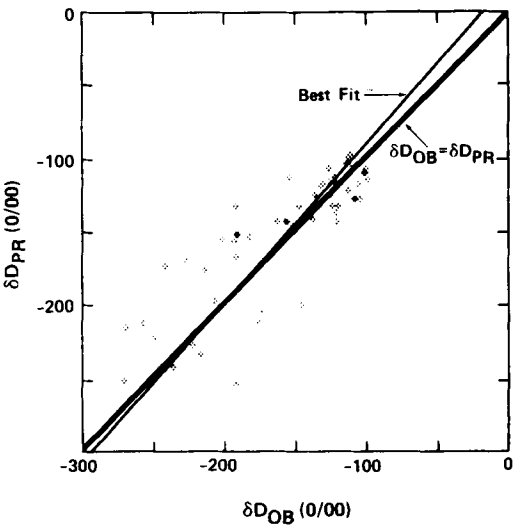

Fig. 13. Same as Fig. 12 for points from unstable or cyclonic soundings. Here actual δD values are compared to predicted values using the fully mixed run with $A = 0$.

fully mixed run with $A = 0$ are shown in Fig. 13. For this case the Rayleigh condensation model gives the best results, although the results for $A = 0.1$ are almost as good. The greater scatter of points about the predicted curve for these unstable soundings is a natural consequence of the more turbulent state of unstably stratified soundings. There is, on average, a small positive bias due mainly to the overprediction of source

vapor δD values at Scottsbluff, which is located well inland and is elevated. The predicted variability of δD values is only slightly larger than observed. The overall success of the fully mixed run supports the applicability of Eriksson's (1965) work to individual situations.

5. Summary and conclusions

Isotopic values of atmospheric water vapor were obtained from two series of flights conducted by Taylor (1972) and Ehhalt (1974) at a number of locations. In this paper we presented a simple model that simulates the δD values for most weather situations. The new feature of the model in this paper and the one which makes it useful in the calculation of actual profiles of δD is that it reconstructs a reasonable trajectory for each air parcel, based only on the sounding data, that takes into account the effect of the degree of subsaturation.

If more accurate δD predictions are needed, it is further necessary to calculate actual air trajectories and have detailed knowledge of the cloud microphysical state and processes, and turbulent and radiative processes all along this trajectory as well as the initial specific humidity and δD values of the vapor. The approach used in this paper was taken because such information was not available for the existing data sets. When large discrepancies between predicted and observed δD values do occur, they yield valuable information regarding meteorological processes that have taken place within the parcel such as:

(1) When predicted δD values are too high then either the initial δD value was assumed too high or the amount of condensation was underestimated. Trajectory analysis will then indicate if a significant fraction of the vapor derived from an inland source of markedly lower δD than the ocean such as the Great Lakes. If there is no such apparent source then the discrepancies between predicted and observed δD values can be used to estimate the amount of radiative cooling that has taken place.

(2) When predicted δD values are too low in an anomalously dry layer then there has been a significant addition of vapor from the surroundings. Eq. (4) or Fig. 5 will then provide an estimate of the vapor content of the dry layer prior to any mixing.

(3) When the atmosphere is undergoing cyclonic scale ascent (prior to condensation) or is neutrally or unstably stratified (we used the criterion, SSI < 2) the vertical gradient of δD values is much reduced. This is due to the vertical turbulent transport of vapor that has not suffered much condensation and fractionation. Under such conditions, model predictions are still useful once, as Eriksson (1965) suggested, the fractionation factor, α, is replaced by $\alpha^{0.5}$.

(4) When an anomalously humid layer in the mid or upper troposphere has a δD value characteristic of air near ground level, it indicates that fractionation processes were not acting normally and that significant reevaporation of hydrometeors occurred. Such layers probably derived from outflow from convective clouds. Since these layers can retain their identity for hundreds of kilometers downwind δD can, on occasion, serve as a tracer of atmospheric motions.

There are also times that the neglect of the cloud microphysics is most likely responsible for any significant discrepancy between predicted and observed δD values. Thus, for example, when predicted δD values are too low, one possibility is that a greater percentage of liquid water was retained in the cloud than was assumed in the model. Therefore, some information about cloud microphysics is potentially retrievable from isotopic measurements. Nevertheless, a one-dimensional model cannot provide reliable quantitative estimates of such important effects as equilibration between the vapor and raindrops falling from above. We are now developing a two-dimensional model that incorporates this and other similar effects so that we can realistically relate δD values to cloud microphysical processes. Further progress in the isotope-weather field hinges on the development of such improved models and the simultaneous collection of isotope and cloud microphysical data.

6. Acknowledgements

I would like to thank Dr. Jean Jouzel of the Laboratoire de Geochimie Isotopique DPC CEN Saclay, France, Dr. James White of Lamont and Dr. James Lawrence of the University of Houston for their many helpful discussions. It is

from these scientists that I have learned much about the isotope field. The comments of several anonymous reviewers were also quite helpful and led to a marked improvement of the paper. The research was supported by NSF ATM grants 81 16371 and 83 13954. Lamont-Doherty Geological Observatory of Columbia University Contribution No. 4198.

REFERENCES

Covey, C. and Haagenson, 1984. A model of oxygen isotope composition of precipitation: implications for paleoclimatic data. *J. Geophys. Res. 83, D3*, 4647–4655.

Dansgaard, W. 1953. The abundance of O^{18} in atmospheric water and water vapour. *Tellus 5*, 461–469.

Dansgaard, W. 1954. The O^{18} abundance in fresh water. *Geochim. Cosmochim. Acta 6*, 241–260.

Dansgaard, W. 1964. Stable isotopes in precipitation. *Tellus 16*, 436–468.

Ehhalt, D. 1974. Vertical profiles of HTO, HDO, and H_2O in the troposphere. NCAR Technical Note, NCAR-TN/STR-100, 131 pp.

Ehhalt, D., Patz, H. W., Pollock, W., Heidt, L. E. and Lueb, R. 1980. Measurement of atmospheric water vapor by cryogenic collection. In: *Atmospheric water vapor*, A. Deepak, T. D. Wilkerson and L. H. Ruhnke, Eds., Academic Press, 303–314.

Eriksson, E. 1965. Deuterium and ^{18}O in precipitation and other natural waters: some theoretical considerations. *Tellus 27*, 498–512.

Facy, L., Merlivat, L., Nief, G. and Roth, R. 1963. The study of formation of hailstones by isotopic analysis. *J. Geophys. Res. 68*, 3841–3848.

Fleagle, R. G. and Businger, J. A. 1980. *An Introduction to Atmospheric Physics*. Academic Press, NY, 432 pp.

Gedzelman, S. D. and Lawrence, J. R. 1982. The isotopic composition of cyclonic precipitation. *J. Appl. Meteorol. 21*, 1385–1404.

Jouzel, J. 1979. Teneur isotopique de la vapeur d'eau atmospherique. Mise au point d'un systeme embarquable. *J. Rech. Atmos. 13*, 261–269.

Jouzel, J. and Merlivat, L. 1984. Deuterium and oxygen-18 in precipitation: modeling of the isotopic effects at snow formation. *J. Geophys. Res. 80*, 5015–5030.

Knight, C. A., Knight, N. C. and Kime, K. A. 1981. Deuterium content of storm inflow and hailstone growth layers. *J. Atmos. Sci. 38*, 2485–2499.

Liu, S. C., McAfee, J. R. and Cicerone, R. J. 1984. Radon 222 and tropospheric vertical transport. *J. Geophys. Res. 89, D5*, 7291–7297.

Majoube, M. 1971. Fractionation of oxygen 18 and of deuterium between water and its vapor (in French). *J. Chim. Phys. 68*, 1423–1436.

Mason, B. J. 1971. *The physics of clouds*, 2nd edition. Oxford University Press, NY, 671 pp.

Merlivat, L. and Jouzel, J. 1979. Global climatic interpretation of the deuterium–oxygen 18 relationship for precipitation. *J. Geophys. Res. 84*, 5029–5033.

Merlivat, L. and Nief, G. 1967. Isotopic fractionation of the solid–vapor and liquid–vapor changes of state of water at temperatures below 0°C (in French). *Tellus 19*, 122–127.

Miyake, Y., Matsubaya, O. and Nishihara, C. 1968. An isotopic study on meteoric precipitation. *Pap. Meteorol. Geophys. 19*, 243–266.

Pollock, W., Heidt, L. E., Leub, R. and Ehhalt, D. H. 1980. Measurement of stratospheric water vapor by cryogenic collection. *J. Geophys. Res. 85*, 5555–5568.

Pruppacher, H. R. and Klett, J. D. 1980. *Microphysics of clouds and precipitation*. D. Riedel Pub. Co., Dordrecht, Holland, 714 pp.

Rozanski, K. and Sonntag, C. 1982. Vertical distribution of deuterium in atmospheric water vapor. *Tellus 34*, 135–141.

Rozanski, K., Sonntag, C. and Münnich, K. O. 1982. Factors controlling stable isotope composition of European precipitation. *Tellus 34*, 142–150.

Taylor, C. B. 1972. The vertical variations of the isotopic concentrations of tropospheric water vapour over continental Europe and their relationship to tropospheric structure. N.Z. Dep. Sci. Ind. Res., Inst. Nucl. Sci., Rep. INS-R-107, 44 pp.

Taylor, C. B. 1984. Vertical distribution of deuterium in atmospheric water vapour: problems in application to assess atmospheric models. *Tellus 36B*, 67–72.

White, J. W. C. and Gedzelman, S. D. 1984. The isotopic composition of atmospheric water vapor and the concurrent meteorological situation. *J. Geophys. Res. 89, D3*, 4937–4939.